01 Aug 2023

Distinct Modes Of Aged Soil Carbon Export In A Large Tropical Lake Basin Identified Using Bulk And Compound-Specific Radiocarbon Analyses Of Fluvial And Lacustrine Sediment

Wesley G. Parker

Jason M.E. Ahad

Jonathan Obrist-Farner
Missouri University of Science and Technology, obristj@mst.edu

Benjamin Keenan

et. al. For a complete list of authors, see https://scholarsmine.mst.edu/geosci_geo_peteng_facwork/2200

Recommended Citation

W. G. Parker et al., "Distinct Modes Of Aged Soil Carbon Export In A Large Tropical Lake Basin Identified Using Bulk And Compound-Specific Radiocarbon Analyses Of Fluvial And Lacustrine Sediment," *Journal of Geophysical Research: Biogeosciences*, vol. 128, no. 8, article no. e2023JG007515, American Geophysical Union; Wiley, Aug 2023.
The definitive version is available at https://doi.org/10.1029/2023JG007515

JGR Biogeosciences

RESEARCH ARTICLE
10.1029/2023JG007515

Key Points:

- ^{14}C data indicate a large proportion of organic matter (OM) and fatty acids in Guatemalan river sediments are derived from old soil carbon
- In different river catchments we find evidence for aged carbon input from either eroded mineral soils or swamp peat
- Lake sediment ^{14}C ages are similar to river values, implying aged soil carbon exported by rivers is buried in lake sediments

Supporting Information:

Supporting Information may be found in the online version of this article.

Correspondence to:

P. M. J. Douglas,
peter.douglas@mcgill.ca

Citation:

Parker, W. G., Ahad, J. M. E., Obrist-Farner, J., Keenan, B., & Douglas, P. M. J. (2023). Distinct modes of aged soil carbon export in a large tropical lake basin identified using bulk and compound-specific radiocarbon analyses of fluvial and lacustrine sediment. *Journal of Geophysical Research: Biogeosciences*, *128*, e2023JG007515. https://doi.org/10.1029/2023JG007515

Received 4 APR 2023
Accepted 2 AUG 2023

Author Contributions:

Conceptualization: Wesley G. Parker, Benjamin Keenan, Peter M. J. Douglas
Data curation: Peter M. J. Douglas
Formal analysis: Wesley G. Parker, Peter M. J. Douglas
Funding acquisition: Wesley G. Parker, Jason M. E. Ahad, Jonathan Obrist-Farner, Peter M. J. Douglas
Investigation: Wesley G. Parker, Jonathan Obrist-Farner, Benjamin Keenan

Distinct Modes of Aged Soil Carbon Export in a Large Tropical Lake Basin Identified Using Bulk and Compound-Specific Radiocarbon Analyses of Fluvial and Lacustrine Sediment

Wesley G. Parker[1], Jason M. E. Ahad[2], Jonathan Obrist-Farner[3], Benjamin Keenan[1], and Peter M. J. Douglas[1]

[1]Department of Earth and Planetary Sciences, Geotop Research Center, McGill University, Montréal, QC, Canada, [2]Geological Survey of Canada, Natural Resources Canada, Québec City, QC, Canada, [3]Department of Geosciences, Geological and Petroleum Engineering, Missouri University of Science and Technology, Rolla, MO, USA

Abstract The ^{14}C content of sedimentary organic matter (OM) and specific organic molecules provide valuable information on the source and age of OM stored in sediments, but these data are limited for tropical fluvial and lake sediments. We analyzed ^{14}C in bulk OM, palmitic acid (C_{16}), and long-chain *n*-alkanoic acids (C_{24}, C_{26}, and C_{28}), within fluvial and lake sediments in the catchment of Lake Izabal, a large tectonic lake basin in Guatemala. We combined these measurements with bulk and compound-specific $\delta^{13}C$ measurements, as well as sediment organic carbon to nitrogen (OC:N) ratios, to understand the source and age of sedimentary OM in different regions of the lake catchment. Most fatty acid and bulk OM samples were characterized by pre-modern carbon, indicating important input of aged carbon with residence times of hundreds to thousands of years into sediments. We identified two mechanisms leading to aged carbon export to sediments. In the high-relief and deforested Polochic catchment, older OM and fatty acids are associated with low % total organic carbon (TOC) and low OC:N, indicating aged OM associated with eroded mineral soil. In the smaller, low-relief, and largely forested Oscuro catchment, old OM and fatty acids are associated with high %TOC and high OC:N ratios, indicating export of undegraded aged plant biomass from swamp peat. The age of bulk OM and fatty acids in Lake Izabal sediments is similar to the ages observed in fluvial sediments, implying that fluvial input of aged soil carbon makes an important contribution to lake sediment carbon reservoirs in this large tropical lake.

Plain Language Summary To understand how carbon stored in lake sediments relates to the global carbon cycle, we need to understand where that carbon is coming from. We analyzed radiocarbon in organic matter from river and lake sediments within a large tropical lake basin in Guatemala to better understand how much carbon was coming from old soil carbon reservoirs. We found that a significant proportion of the carbon exported by the rivers to the lake came from old soil carbon. We found that the mechanism leading to this soil carbon export was different in two different river catchments. In a mountainous and deforested river catchment the old carbon was derived from erosion of upland soils, whereas in a lowland forested river catchment the old carbon was derived from peat stored in swamps. Our results indicate that the old carbon exported by rivers is buried in lake sediments, with more of the lake sediment carbon coming from upland soil erosion. This implies that in this large tropical lake basin much of the carbon buried in lake sediments is derived from old soil carbon, representing an efficient transfer of carbon from one long-term carbon reservoir to another.

1. Introduction

Freshwater sediments are a globally important carbon reservoir that remains poorly characterized in terms of its overall size, the source of the carbon it stores, and its sensitivity to climatic and environmental change (Anderson et al., 2020; Dean & Gorham, 1998; Mendonça et al., 2017). A recent study estimated that approximately 0.15 Pg of organic carbon (OC) is buried in freshwater sediments annually (Mendonça et al., 2017), but the role of freshwater carbon burial in the global carbon cycle and how this sink may change with time remains uncertain (Regnier et al., 2022). Soil erosion is also an important process controlling the long-term fate of terrestrial carbon reservoirs, and much of the carbon in eroded soils is likely redistributed to aquatic sediments (Berhe et al., 2007; Tan et al., 2020; Wang et al., 2017). However, the contribution of soil organic matter (OM) to fresh-

Methodology: Wesley G. Parker, Jason M. E. Ahad, Jonathan Obrist-Farner, Benjamin Keenan
Project Administration: Peter M. J. Douglas
Resources: Jason M. E. Ahad, Jonathan Obrist-Farner
Supervision: Jason M. E. Ahad, Jonathan Obrist-Farner, Peter M. J. Douglas
Visualization: Wesley G. Parker, Peter M. J. Douglas
Writing – original draft: Wesley G. Parker, Peter M. J. Douglas
Writing – review & editing: Wesley G. Parker, Jason M. E. Ahad, Jonathan Obrist-Farner, Peter M. J. Douglas

water sediments remains loosely defined, especially in terms of empirical studies at the scale of ecosystems or catchments, and especially in the tropics.

Radiocarbon measurements of OM in aquatic sediments are a powerful tool for identifying the input of aged soil OM transported to inland water and coastal ecosystems (Copard et al., 2022; Griffith et al., 2010; McCorkle et al., 2016; Vonk et al., 2010a). In particular, compound-specific radiocarbon measurements of long-chain fatty acids, or leaf waxes, have been widely used as an indicator of the mean age or transit time of plant-derived carbon in sediments (Douglas et al., 2014; Galy & Eglinton, 2011; Vonk et al., 2019). Leaf-wax radiocarbon ages in large river catchments are linked to global-scale variability in soil carbon residence time (Eglinton et al., 2021), and have been used to trace changes in soil carbon storage related to climatic or anthropogenic environmental change (Douglas et al., 2018; Gierga et al., 2016; Hein et al., 2020; Schefuß et al., 2016). Additionally, short-chain fatty acids such as palmitic acid are produced by a wider range of organisms, including microbes and algae, but their ^{14}C measurements can likewise be a valuable indicator of the mean age or transit time of labile organic molecules, including microbial biomass (Grant et al., 2022; Makou et al., 2018).

Compound-specific radiocarbon data for fatty acids are relatively rare in tropical river catchments, and are largely limited to a few large river systems, such as the Congo, Pearl, and Ganges-Brahmaputra Rivers (Galy & Eglinton, 2011; Hein et al., 2020; Schefuß et al., 2016; Wei et al., 2021). In general, the available data imply that soil carbon residence times in the humid tropics are relatively short, largely because of high temperatures and precipitation that promote both rapid decomposition and flushing of soil OM (Eglinton et al., 2021). Gathering data from a broader range of tropical ecosystems is important given that tropical soils are a large carbon reservoir, and because anthropogenic deforestation and climate change can destabilize these reservoirs and release long-stored soil carbon (Douglas et al., 2018; Gierga et al., 2016; Hein et al., 2020; Schefuß et al., 2016). Most available data are from the mouths of large river systems, and there are very limited data available to analyze how OM and fatty acid ^{14}C ages vary across a fluvial network, or how they differ between river and lake sediments. Spatially resolved data would help to resolve environmental variables that promote the export of aged soil carbon to fluvial systems, and to understand the extent to which this aged carbon is buried in lake sediments.

Stable isotope ratios of long-chain fatty acids and other leaf wax lipids preserved in sediments are also widely applied as a paleoclimate proxy for changes in hydroclimate or vegetation (Diefendorf & Freimuth, 2017; Inglis et al., 2022; Sachse et al., 2012). However, the phenomenon of pre-aged leaf waxes in freshwater and coastal sediments likely poses complications for the interpretation of leaf wax isotope records, at least on millennial and shorter timescales (Douglas et al., 2014; Freimuth et al., 2021; French et al., 2018). There are relatively few data from lake sediments that can be used to understand patterns in the soil residence time of plant wax lipids. Available data imply that centennial to millennial age offsets between plant wax ^{14}C ages and the age of sediment deposition are common (Aichner et al., 2021; Freimuth et al., 2021; Gierga et al., 2016; Yamamoto et al., 2020), but there is no clear indication of geomorphological or ecological variables that control variation in these offsets. There are only a few data sets from tropical lake sediments, which generally point to age offsets between 200 and 1,000 years (Douglas et al., 2014; Kruger et al., 2022; Uchikawa et al., 2008). However, many of these data are from small lakes in karst basins, and more data from larger lakes and from different geomorphological settings is needed to determine the pervasiveness of these offsets. Likewise, comparing ^{14}C ages in sediments throughout a lake catchment would be helpful in identifying if there is substantial mixing of plant waxes and other fatty acids with different soil residence times in lake sediment archives.

In this study, we develop new insights into the export of aged OM and fatty acids from soils to sediments in a large tropical lake basin, the Lake Izabal Basin (LIB) located in eastern Guatemala. Lake Izabal is the largest lake in Guatemala, and is fed by a large and complex network of rivers (Obrist-Farner et al., 2020). Lake Izabal also contains a deep sedimentary record that spans millions of years, and could be a valuable repository of paleoclimate data (Bartole et al., 2019; Duarte et al., 2021; Obrist-Farner et al., 2022, 2023), including reconstructions based on leaf wax isotope data. We sampled sediments from across the LIB, including three major rivers that feed the lake, as well as the lake itself and marshes adjacent to the Polochic river delta. We analyzed the ^{14}C content of bulk OM, short-chain fatty acids (C_{16}), and long-chain fatty acids (C_{24}, C_{26}, and C_{28}). This approach allows us to compare the age of different fractions of OM across this complex landscape and assess key mechanisms and geographic patterns of aged carbon export. Particular questions we seek to answer include: (a) Is there a difference in the age of OC in high-relief upland rivers and low-relief lowland rivers?; (b) Is there a difference in the age of carbon between a large river catchment with intensive land use, and a smaller catchment that remains

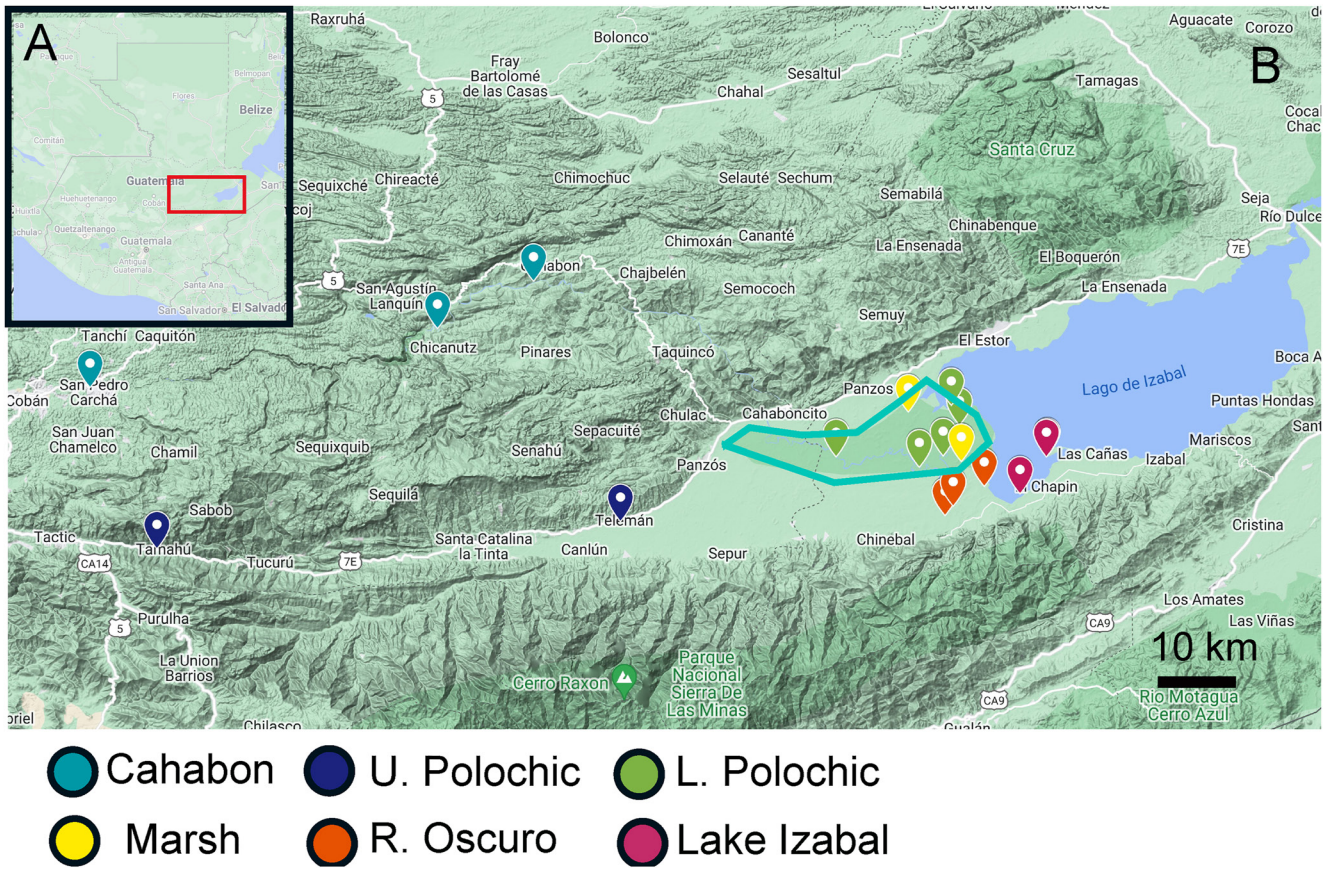

Figure 1. Maps showing (a) the location of the Lake Izabal catchment in Guatemala, (b) the location of sampling sites relative to local relief. The cyan polygon indicates the approximate extent of the Bocas del Polochic wetland. Base maps from Google Maps.

largely forested?; (c) Are there substantial and systematic differences in age between the three studied carbon fractions that reflect their differing recalcitrance and sources?; and (d) Is the age of OC in lake sediments representative of that found in upstream river sediments?

2. Geographical, Geological, and Climatic Setting

The LIB is a tectonically-active pull-apart basin that formed ~12 Myr ago along the Polochic-Motagua Fault System (Obrist-Farner et al., 2020), which denotes the inland extension of the Caribbean/North American plate boundary (Bartole et al., 2019) (Figure 1). Lake Izabal is a shallow (15 m maximum water depth), hydrologically open lake which sits near sea level (2 m above sea level) and is connected to the Caribbean Sea through the Dulce River (Brinson et al., 1974).

The primary source waters for Lake Izabal are the Polochic and Cahabón Rivers, which originate west and northwest of Lake Izabal, respectively, and together comprise the Polochic Watershed (PW), which drains an area of ~8,400 km^2 (Obrist-Farner et al., 2019). The 180-km-long Cahabón River is the larger of the two rivers that comprise the PW and originates within the nearby Santa Cruz Mountain Range (Figure S1 in Supporting Information S1). It is one of the largest rivers in Guatemala by volume, with an average discharge of 164.2 m^3/s (INSIVUMEH, 2022). The 194-km-long Polochic River is smaller by volume, with an average discharge of 69.3 m^3/s (INSIVUMEH, 2022). The Polochic River originates in the Polochic Valley between the Santa Cruz and Sierra de las Minas mountain ranges, and its largest tributary is the Cahabón River, with the junction of the two rivers approximately 36 km west of the point where the Polochic River drains into Lake Izabal. The two rivers pass through multiple geologic provinces before draining into Lake Izabal (Bonis et al., 1970). Most rocks exposed in the Cahabón Valley are Mesozoic carbonate rocks, while Paleozoic carbonate, clastic, and metamorphic rocks are exposed along the Polochic Valley (Figure S2 in Supporting Information S1). After the

confluence of the Cahabón River, the Polochic River passes through a low-relief marsh, the Bocas del Polochic wetland, before its final discharge into the western margin of Lake Izabal (Figure 1; Figure S3 in Supporting Information S1).

The significantly smaller Oscuro Watershed (OW) drains an area of 233 km^2, adjacent to and southeast of the PW. The OW represents a secondary input into Lake Izabal, and centers geographically around the Oscuro River, which originates southwest of the lake. The Oscuro River has a length of 10 km, and discharge is highly variable, but is approximately 62 m^3/s on average (Brinson, 1976). The majority of the drainage basin for the OW is comprised of lowland swamp forest (Figure S4 in Supporting Information S1), which overlies alluvial sediments (Brinson, 1976). Unlike the rivers of the PW, the majority of the OW catchment remains waterlogged or flooded year-round, and the overflow of the Polochic river during wet-season flooding often transfers water and sediments into the OW (Brinson, 1976). This, along with low topographic relief, contributes to an imprecise delineation of the boundary between the OW and PW and the watersheds are considered to be partially inter-connected.

Data from a meteorological station in the Izabal region indicate that the region experiences a two-season monsoon climate, with an annual mean precipitation of 3,321 mm (Duarte et al., 2021; INSIVUMEH, 2022). Average annual temperature is 26°C, and varies by approximately 6° over the course of the year (Duarte et al., 2021). Local vegetation zones include lowland moist forests, montane forests, and pine-oak forests, in addition to agricultural areas, primarily subsistence maize agriculture or milpa (Olson et al., 2001). Vegetation regimes across the LIB and PW are predominantly controlled by local precipitation, topography, and elevation. The PW is subject to extensive anthropogenic disturbance, including deforestation and agriculture (Figure S2 in Supporting Information S1), while the OW is more pristine (Brinson, 1976), although both watersheds and the greater LIB contain well-established anthropogenic impacts (Obrist-Farner et al., 2019).

3. Materials and Methods

3.1. Field Sampling Methods

Surface sediments from Lake Izabal and from the Polochic, Cahabón, and Oscuro rivers were collected either using an AMS Ekman Dredge for fluvial sediments or a sediment-water interface corer for lake sediments in July 2017. For the dredged samples, we collected approximately the uppermost 5–10 cm of sediment. Surface sediments in Lake Izabal were collected using a piston corer designed for the retrieval of undisturbed mud-water interface deposits (Fisher et al., 1992) (Figure S5 in Supporting Information S1). The uppermost 3 cm of the mud-water interface core were placed in Whirl-Pak™ bags and stored. Based on age-depth models from dated sediment cores in Lake Izabal (Hernández et al., 2020; Obrist-Farner et al., 2019) we infer this represents approximately 5 years of sediment deposition. The sampling locations (Table S1 in Supporting Information S2; Parker et al., 2023) were determined based on access to the rivers and the lake, as well as to achieve a sample set representative of the Lake Izabal catchment. Sediments were stored in a cool box in the field, transferred to a refrigerator, and stored at 2°C for up to 2 weeks before being frozen.

3.2. Bulk Sediment Elemental and Isotopic Analyses

Freeze-dried sediments were homogenized using a mortar and pestle, and two small aliquots were removed for total organic carbon (TOC), total nitrogen (TN), and bulk sediment radiocarbon and carbon-13 analyses. The first aliquot was analyzed at the GEOTOP stable isotope laboratory at the Université du Québec à Montréal for TOC, TN, and bulk OM $\delta^{13}C$ analyses. Freeze-dried samples were carefully weighed, and then acid fumigated with HCl vapor for 24 hr to remove inorganic carbon. One sample aliquot was then analyzed for TOC (wt%) and TN (wt%) and a second aliquot analyzed for bulk OM $\delta^{13}C$. Analytical uncertainty was ±0.07% for TOC and ±0.01% for TN. The samples were analyzed with a Micromass Isoprime 100 Isotope Ratio Mass Spectrometer coupled to an Elementar Vario MicroCube elemental analyzer (EA) in continuous flow mode. $\delta^{13}C$ results are expressed as ‰ deviations from the Vienna Pee Dee Belemnite (VPDB) standard in conventional delta notation (Coplen, 2011). Two internal reference materials ($\delta^{13}C = -28.73‰$ and $-11.85‰$) were used to normalize the results on the NBS19-LSVEC scale, and a third reference material ($\delta^{13}C = -17.04‰$) was analyzed as an unknown. The overall analytical uncertainty (1σ) for $\delta^{13}C$ is better than ±0.1‰.

A second aliquot from each sample was analyzed at the A.E. Lalonde Accelerator Mass Spectrometry Laboratory at the University of Ottawa for bulk OM $\Delta^{14}C$ analysis. Samples were acid washed in HCl (1 N, 80°C, 30 min)

to remove inorganic carbon. The samples were weighed in tin cups, combusted to CO_2 using a Thermo Flash 1112 EA, and the CO_2 was cryogenically separated in a breakseal. Blank tin capsules were combusted between each sample to monitor the blank and to ensure no memory effect. The breakseals, containing grains of silver cobaltous, were baked at 200°C to remove sulfur and halogens. The CO_2 in the breakseals was reduced to graphite in the presence of Fe-H. The ^{14}C content of the resulting graphite was analyzed on a 3MV tandem accelerator mass spectrometer (AMS), and the results were background corrected. Fraction modern carbon (Fm) was calculated as the ratio of the sample $^{14}C/^{12}C$ to the standard $^{14}C/^{12}C$ ratio (Reimer, 2004). Both $^{14}C/^{12}C$ ratios are background-corrected and the result was corrected for spectrometer and preparation fractionation using the AMS measured $^{13}C/^{12}C$ ratio and is normalized to $\delta^{13}C$. The typical analytical uncertainty for bulk OM Fm values was ±0.003.

3.3. Lipid Extraction

Between 8.8 and 191.3 g of dried sediments were solvent extracted in 9:1 dichloromethane (DCM) and methanol (MeOH) for 30 min at 80°C using a CEM (Matthews, NC) MARSXpress microwave solvent extractor. Following extraction, the total lipid extract (TLE) was centrifuged, pipetted into evaporation tubes, and evaporated under a continuous N_2 flow at 40°C until dry to remove all solvents. The TLE was then flushed through sodium sulfate in Pasteur pipettes using 15 mL of MeOH and 15 mL of DCM to remove water. The TLE was then saponified in 5 mL of 1 M KOH in MeOH at 80°C for 2 hr, combined with 5 mL 5% NaCl in distilled water, and then extracted with a 2:1 mixture of hexane and DCM to yield the neutral fraction. The pH of the remaining saponified extract was reduced to <1 with 1 M HCl and was again extracted with 2:1 hexane and DCM to yield the acid fraction. The neutral fraction was evaporated and reserved for future studies. The acid fraction was derivatized using 14% BF_3 in MeOH (80°C for 30 min). The resulting fatty acid methyl esters (FAMEs) were combined with 5 mL 5% NaCl in distilled water, extracted with 2:1 hexane and DCM, and dehydrated via elution through a second $NaSO_4$ column. Purified FAMEs were quantified relative to laboratory FAME standards (SUPELCO) using a Thermo Trace 1350 Gas Chromatograph with a Flame Ionization Detector (GC-FID) with a 60 m Thermo TG-5 column, using He as the carrier gas.

3.4. Compound-Specific Radiocarbon Analysis

Specific FAMEs (C_{16}, C_{24}, C_{26}, and C_{28}) were isolated by preparative capillary gas chromatography (PCGC) at the Geological Survey of Canada's Delta Lab (GSC-Québec). The system employs an Agilent (Santa Clara, CA, USA) 7890A gas chromatograph equipped with two 30 m × 0.53 mm × 0.5 µm ZB-5 columns (Phenomenex Inc., Torrance, CA) and a flame ionization detector (FID) coupled to a Gerstel (Linthicum, MD, USA) preparative fraction collector. Targeted FAMEs were collected in pre-combusted (450°C for 4 hr) glass U-traps using similar PCGC conditions to those outlined in Ahad et al. (2012) and Ahad and Pakdel (2013). Individual FAME abundances and purity were quantified and assessed using an Agilent gas chromatograph—mass spectrometer (GC-MS) system (GC 7890A and a 5975C mass selective detector) equipped with a 30 m × 0.25 mm × 0.25 µm Z B-5MSplus column (Phenomenex Inc.).

All sample sites yielded sufficient C_{16} for compound-specific radiocarbon analysis (CSRA). However, abundances of individual long-chain FAMEs were insufficient for individual ^{14}C analysis at sites LIM 7, 9, 11, 12, and 18. Accordingly, at these sites three long-chain *n*-alkanoic acid homologs (C_{24}, C_{26}, and C_{28}) were combined. Additionally, all long-chain *n*-alkanoic acid homologs were combined across multiple samples from sites LIM 3, 25, 26 and 27, creating a multi-sample composite measurement for the Lower Polochic subregion, due to insufficient long-chain FAME abundances within the individual samples. Purified FAME samples, the MeOH used for esterification, and two laboratory ^{14}C standards (see below) were sent to the National Ocean Sciences Accelerator Mass Spectrometry (NOSAMS) Facility at Woods Hole Oceanographic Institution for CSRA. The samples were transferred to pre-combusted quartz tubes and all solvent was evaporated under nitrogen. Precombusted cupric oxide was added to the tubes, which were then flame-sealed under vacuum and combusted at 850 C for 5 hr. The resulting CO_2 was quantified and purified on a vacuum line, and then reduced to graphite and analyzed for radiocarbon content using the NOSAMS AMS. The ^{14}C content of the resulting graphite was analyzed on a 500 kV pelletron AMS, and the results were background corrected. Fraction modern carbon (Fm) was calculated as the ratio of the sample $^{14}C/^{12}C$ to the standard $^{14}C/^{12}C$ ratio (Reimer, 2004). Both $^{14}C/^{12}C$ ratios are background-corrected and the result is corrected for spectrometer and preparation fractionation using the AMS measured $^{13}C/^{12}C$ ratio. The typical analytical uncertainty for compound-specific Fm values was ±0.006.

Compound-specific radiocarbon ^{14}C data for *n*-alkanoic acids were corrected for the isotopic composition of the carbon from the methyl group added during esterification, following the procedures outlined in Douglas et al. (2014). The methanol did not contain measurable ^{14}C. The $\Delta^{14}C_{acid}$ was calculated using the following equation:

$$\Delta^{14}C_{acid} = \frac{\left((n+1) \times \Delta^{14}C\right) + 1,000}{n} \quad (1)$$

where n is equal to the weighted average of the chain-lengths (number of carbon atoms) in the original, non-methylated compound(s) analyzed. All radiocarbon data are primarily reported as Fm values, which in the case of compound-specific radiocarbon samples were calculated from methanol-corrected $\Delta^{14}C_{acid}$ values. To assess for potential contamination introduced during PCGC separation and collection, two in-house ^{14}C standards were processed following the same protocols used for samples. The two in-house standards were palmitic acid extracted from a growing maple leaf sampled in Montreal in 2021, which is assumed to have the value of the contemporary atmosphere, and C_{27} *n*-alkane extracted from a Cretaceous mudstone from Saskatchewan (Bourque et al., 2021), which is assumed to contain no detectable ^{14}C. The radiocarbon contents for both the modern and fossil in-house standards were within analytical uncertainty of the expected Fm values (modern Maple leaf C_{16} fatty acid Fm = 0.99 ± 0.007; Cretaceous C_{27} alkane Fm = 0.004 ± 0.003), and therefore no additional correction was applied to the samples. We also analyzed solvent blanks by GC-MS to assess for contamination during wet sample preparation and PCGC, and these solvent blanks did not indicate significant extraneous input of the targeted FAMEs.

3.5. Compound-Specific Stable Isotope Analysis

Compound-specific isotope analyses were conducted to determine FAME $\delta^{13}C$ values for 11 of 18 samples (LIM 7, 9, 11, 12, 13, 15, 16, 17, 25, 26, and 34). Residual FAME abundances following CSRA analysis were too low to analyze FAME $\delta^{13}C$ values from the remaining samples. Analyses were conducted using a Thermo Scientific GC Isolink coupled to a Thermo Delta V isotope ratio mass spectrometer in the McGill University Department of Earth and Planetary Sciences, using a 60 m Thermo TG-5MS column. Resultant $\delta^{13}C$ values were calculated relative to a FAME standard (Mix F8) calibrated to the VPDB scale (Schimmelmann et al., 2016). An internal laboratory FAME standard (Supelco) was analyzed between every three sample runs to characterize measurement uncertainty and instrumental drift. FAME $\delta^{13}C$ values were corrected for the addition of methyl carbon using measurements of phthalic acid with a known isotopic composition derivatized with the same BF_3-MeOH as our samples, as described by Douglas et al. (2014). Carbon isotope values are expressed as ‰ deviations from the VPDB standard in conventional delta notation (Coplen, 2011). Analytical precision, based on internal and external standards is ±0.30‰.

3.6. Mixing Model Calculations

To calculate approximate estimates of the contribution of pre-aged soil carbon to sediments at the river mouths and in Lake Izabal, we used a simple two end-member mixing model based on Fm values. We did not incorporate $\delta^{13}C$ values in the mixing model because of uncertainty in end-member values, and because lake sediment values were distinctly depleted relative to fluvial sediment values.

The mixing model was based on the following equation:

$$Fm_t = (f_s Fm_s) + (f_c Fm_c) \quad (2)$$

where Fm_t is the total Fm value of the measured OM or fatty acid, Fm_s is the Fm value of the aged soil OM endmember, Fm_c is the Fm value for the contemporary biomass endmember, f_s is the fraction of the measured OM or fatty acid derived from aged soil carbon, and f_c is the fraction of the measured OM or fatty acid derived from contemporary biomass. The sum of f_s and f_c is assumed to be 1.

In the absence of direct measurements of catchment soils, we use the oldest fatty acid measurements from a given catchment as an indicator of Fm_s. For the PW this is palmitic acid in the most upstream sample of the Upper Polochic (LIM-41; Fm = 0.82), and for the OW this is leaf waxes from the most upstream sample (LIM-15; Fm = 0.74). For Lake Izabal sediments we use the endmember from the PW, since these sediments are more similar in their bulk geochemistry to PW sediments. For contemporary biomass we use an Fm value of 1.05 in

all catchments, based on the approximate value of northern hemisphere atmospheric CO_2 for the past decade (Turnbull et al., 2017). Given the uncertainties in the end-member values, the mixing model results are for illustrative purposes only, and should not be considered quantitative estimates.

4. Results

4.1. Total Organic Carbon, Nitrogen, and OC:N

TOC, TN, and OC:N results were highly variable (Table 1; Table S1 in Supporting Information S2; Parker et al., 2023). To highlight differences between sampling regions we report mean and standard deviation values for five distinct sampling regions: Upriver Polochic watershed (UPW) (defined as upstream of the Polochic-Cahabón confluence), Downriver Polochic watershed (DPW) (downstream of the Polochic-Cahabón confluence), Polochic Marshes PM (sites located away from the Polochic River), OW, and Lake Izabal sediments LI. TOC and TN distributions for the different regions were highly skewed, leading to large standard deviations. The mean TOC and TN of the five regions is as follows: UPW ($n = 5$) 1.51 ± 2.04% TOC and 0.15 ± 0.15% TN; DPW ($n = 5$) 1.55 ± 0.5% TOC and 0.14 ± 0.05% TN; PM ($n = 2$) 24.3 ± 25% TOC and 1.23 ± 0.89% TN; OW ($n = 3$) 15.13 ± 13.79% TOC and 0.70 ± 0.58% TN; and LI ($n = 3$) 4.88 ± 2.42% TOC and 0.47 ± 0.19% TN. The mean molar OC:N ratios for each subregion were UPW 9.76 ± 3.30; DPW 13.3 ± 0.87; PM 19.77 ± 9.1; OW 25.86 ± 4.83; and LI 11.86 ± 0.90 (Figure 2a).

4.2. Bulk Sediment Radiocarbon

Bulk sediment radiocarbon results are reported as both Fm values (Fm_{OM}) and uncalibrated ^{14}C ages before present (BP) (Table 1). Of 18 samples, 5 contain dominantly modern carbon with an Fm > 1. One age, retrieved from LIM-41 in the Upper Polochic region, is anomalously old (14,455 years BP) when compared to the other samples. The carbon dioxide yield for LIM-41 was within normal range, and the sample measurement was repeated multiple times to ensure that this anomalous age was not due to laboratory error. Further evidence that this is an anomalous sample is the bulk sediment $\delta^{13}C$ value (−22.8‰) which is 2.2‰ higher than the next highest $\delta^{13}C$ value. Possible sources for this anomalous data point could include incorporation of fossil carbon from (a) dolomite or other carbonates rocks; (b) petrogenic OC from sedimentary rocks; or (c) anthropogenic contamination. Because of possible incorporation of detrital dolomite, despite leaching in HCl, we consider the carbon isotope results from this sample to be anomalous and possibly biased.

Excluding LIM-41, the mean Fm_{OM} values for each region are: UPW ($n = 4$) 0.96 ± 0.05 (corresponding to 350 ± 391 ^{14}C years BP); DPW 0.98 ± 0.02 (188 ± 120 ^{14}C years BP); PM 1.06 ± 0.05 (modern); OW 0.95 ± 0.07 (450 ± 584 ^{14}C years BP), and LI 0.98 ± 0.008 (204 ± 67 ^{14}C years BP) (Figure 3a).

4.3. Compound-Specific Radiocarbon

Compound-specific radiocarbon ages are presented as both Fm values and uncalibrated ^{14}C ages before present (BP) (Table 1). The palmitic acid Fm values (FM_{PA}) span from 1.03 to 0.8 (modern to 1825 ^{14}C years BP) with a mean value of 0.94 ± 0.06 (561 ± 513 ^{14}C years BP). Average values for each subregion are: UPW 0.91 ± 0.05 (784 ± 469 ^{14}C years BP); DPW 0.97 ± 0.008 (261 ± 82 ^{14}C years BP); PM 1 ± 0.042 (0 ± 190 ^{14}C years BP); OW 0.88 ± 0.10 (1,042 ± 902 ^{14}C years BP); and LI 0.95 ± 0.03 (473 ± 287 ^{14}C years BP) (Figure 3b).

Because of low abundances and the need to combine long-chain fatty acids in most samples, we focus on the mean Fm (Fm_{LW}) and ^{14}C ages of the three long-chain *n*-alkanoic acid compounds (C_{24}, C_{26}, and C_{28}), or leaf waxes, for all samples (Table 1). Individual leaf wax ^{14}C data for four samples are available in Table S3 in Supporting Information S2 (Parker et al., 2023). For samples where individual FAMEs were analyzed we calculated FM_{LW} as the concentration weighted mean value. The mean Fm_{LW} values for the subregions are: DPW ($n = 2$) 0.91 ± 0.007 (801 ± 95 ^{14}C years BP); PM ($n = 2$) 0.98 ± 0.04 (170 ± 282 ^{14}C years BP); OW 0.86 ± 0.11 ($n = 3$) (1,191 ± 1,082 ^{14}C years BP); and LI ($n = 3$) 0.85 ± 0.1 (1,274 ± 979 ^{14}C years BP) (Figure 3c). There are no Fm_{LW} data for the UPW region due to low concentrations.

4.4. Bulk and Compound-Specific $\delta^{13}C$

Bulk sediment OM $\delta^{13}C$ ($\delta^{13}C_{OM}$) values range from −31.2‰ to −25.0‰, excluding the anomalous sample LIM-41, with an average value of −28.5 ± 1.9‰ (Table 1). Average values for the five subregions are: UPW

Journal of Geophysical Research: Biogeosciences
10.1029/2023JG007515

Table 1
Sample OC:N and Bulk and Compound-Specific $\delta^{13}C$, Fm, and ^{14}C Age Results

Sample ID	Subregion	OC:N molar	$\delta^{13}C_{OM}$ (‰, VPDB)	Fm_{OM}	OM ^{14}C age	$\delta^{13}C_{PA}$ (‰, VPDB)	Fm_{PA}	PA ^{14}C age	$\delta^{13}C_{LW}$ (‰, VPDB)	Fm_{LW}	LW ^{14}C age
LIM-46	Upper Polochic	7.7	−25.8	0.941 (±0.004)	485 (±35)		0.92 (±0.009)	645 (±80)			
LIM-41	Upper Polochic	6.0	−22.8	0.165 (±0.001)	14,450 (±65)		0.82 (±0.01)	1,600 (±110)			
LIM-34	Cahabón	9.0	−27.7	1.022 (±0.004)	–	−31.5	0.91 (±0.009)	725 (±90)	*−33.8*		
LIM-36	Cahabón	11.8	−27.2	0.972 (±0.003)	225 (±25)		0.94 (±0.01)	460 (±90)			
LIM-39	Cahabón	14.3	−25.0	0.893 (±0.004)	910 (±35)		0.94 (±0.009)	490 (±80)			
LIM-3	Lower Polochic	11.6	−25.7	1.010 (±0.003)	–		0.98 (±0.004)	145 (±35)			
LIM-12	Lower Polochic	13.0	−28.1	0.966 (±0.003)	280 (±30)	−30.5	0.97 (±0.004)	275 (±35)	*−32.5*	0.91 (±0.007)	750 (±60)
LIM-25	Lower Polochic	14.0	−28.3	0.974 (±0.004)	210 (±30)	−32.3	0.97 (±0.004)	275 (±35)	*−33.6*		
LIM-26	Lower Polochic	13.0	−27.9	0.971 (±0.003)	235 (±25)	−32.2	0.96 (±0.006)	355 (±55)	*−33.1*		
LIM-27	Lower Polochic	13.4	−27.2	0.963 (±0.003)	300 (±30)		0.96 (±0.01)	335 (±90)			
LIM-13	Polochic Marsh	26.2	−30.5	1.095 (±0.003)	–	−35.4	1.03 (±0.003)	–	*−33.7*	*1.01 (±0.003)*	–
LIM-18	Polochic Marsh	13.4	−30.0	1.018 (±0.003)	–		0.97 (±0.004)	270 (±40)		0.95 (±0.003)	400 (±25)
LIM-15	Oscuro	20.4	−29.5	0.869 (±0.003)	1,130 (±25)	−35.0	0.80 (±0.004)	1,825 (±40)	*−33.6*	*0.74 (±0.003)*	*2,390 (±35)*
LIM-16	Oscuro	27.6	−29.5	1.006 (±0.003)	–	−35.0	0.99 (±0.004)	55 (±30)	*−33.3*	*0.97 (±0.003)*	*250 (±25)*
LIM-17	Oscuro	29.6	−29.9	0.962 (±0.003)	310 (±30)	−34.5	0.86 (±0.006)	1,245 (±55)	*−32.9*	*0.88 (±0.006)*	*1,070 (±60)*
LIM-7	Lake Izabal	12.9	−30.4	0.984 (±0.003)	130 (±25)	−35.6	0.97 (±0.005)	260 (±45)	*−34.7*	0.93 (±0.004)	620 (±30)
LIM-9	Lake Izabal	11.2	−31.2	0.969 (±0.003)	260 (±25)	−35.9	0.91 (±0.007)	800 (±70)	*−34.8*	0.74 (±0.005)	2,450 (±55)
LIM-11	Lake Izabal	11.5	−31.2	0.972 (±0.003)	225 (±30)	−37.1	0.96 (±0.005)	360 (±50)	*−34.4*	0.89 (±0.004)	930 (±35)
Combined samples											
LIM 3, 25, 26, 27									*−33.3*	0.90 (±0.003)	885 (±30)

Note. Italics indicate average value compiled from measurements of multiple compounds. Individual compound data shown in Tables S2 and S3 in Supporting Information S2. LW, Combined leaf wax (C_{24}, C_{26}, and C_{28} fatty acids); PA, Palmitic acid (C_{16} fatty acid); OM, Bulk organic matter.

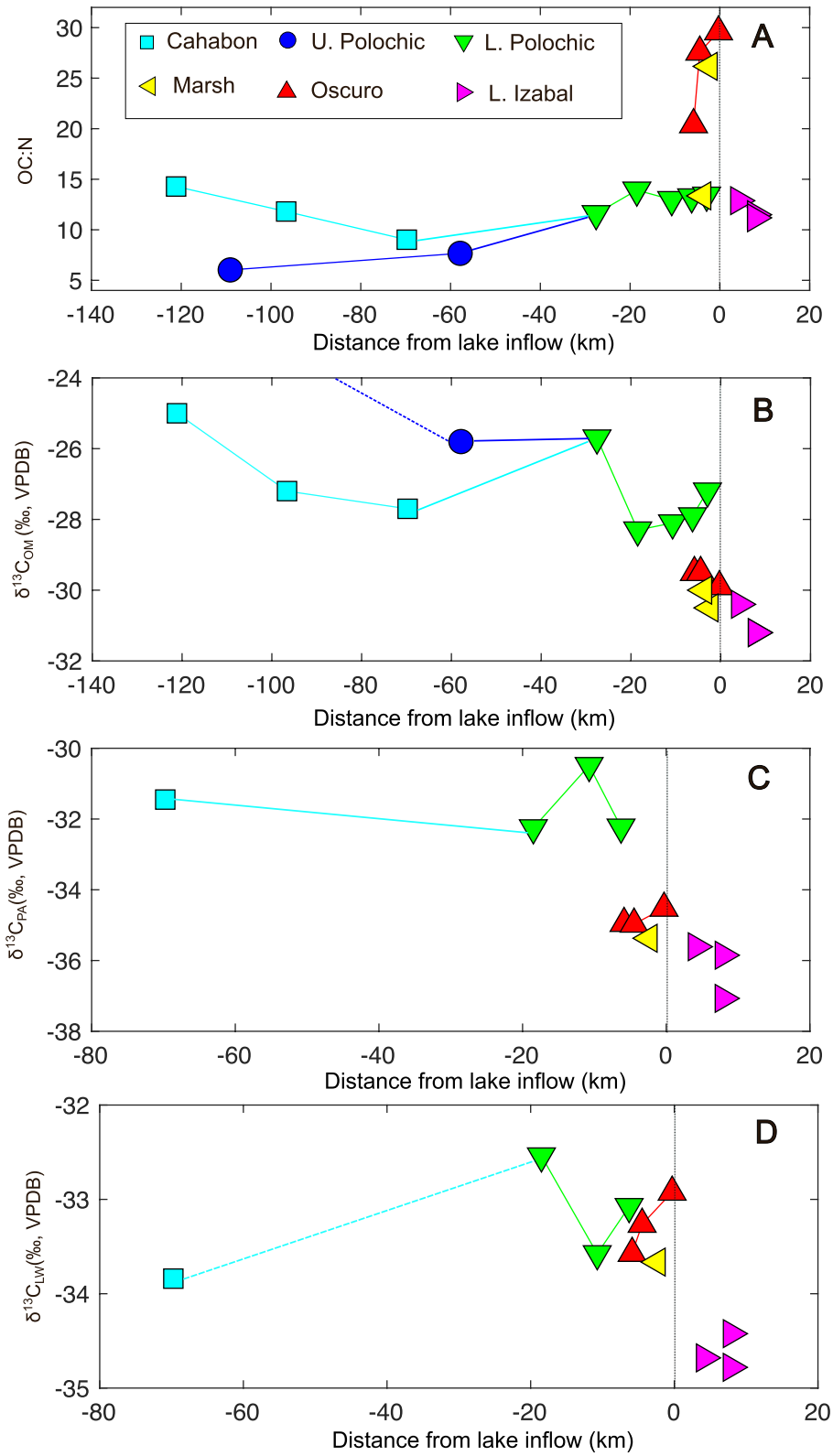

Figure 2. OC:N (a), $\delta^{13}C_{OM}$ (b) $\delta^{13}C_{PA}$ (c), and $\delta^{13}C_{LW}$ (d) as a function of distance from the river mouths entering Lake Izabal. Negative distances are upstream of the lake mouth, and positive distances are offshore of the lake. Dotted blue line in (b) indicates the trend toward anomalous sample LIM-41. The *x*-axis dimensions are different in (c) and (d) because there were no data for the most upstream samples. The analytical uncertainty is smaller than the symbol size for all data.

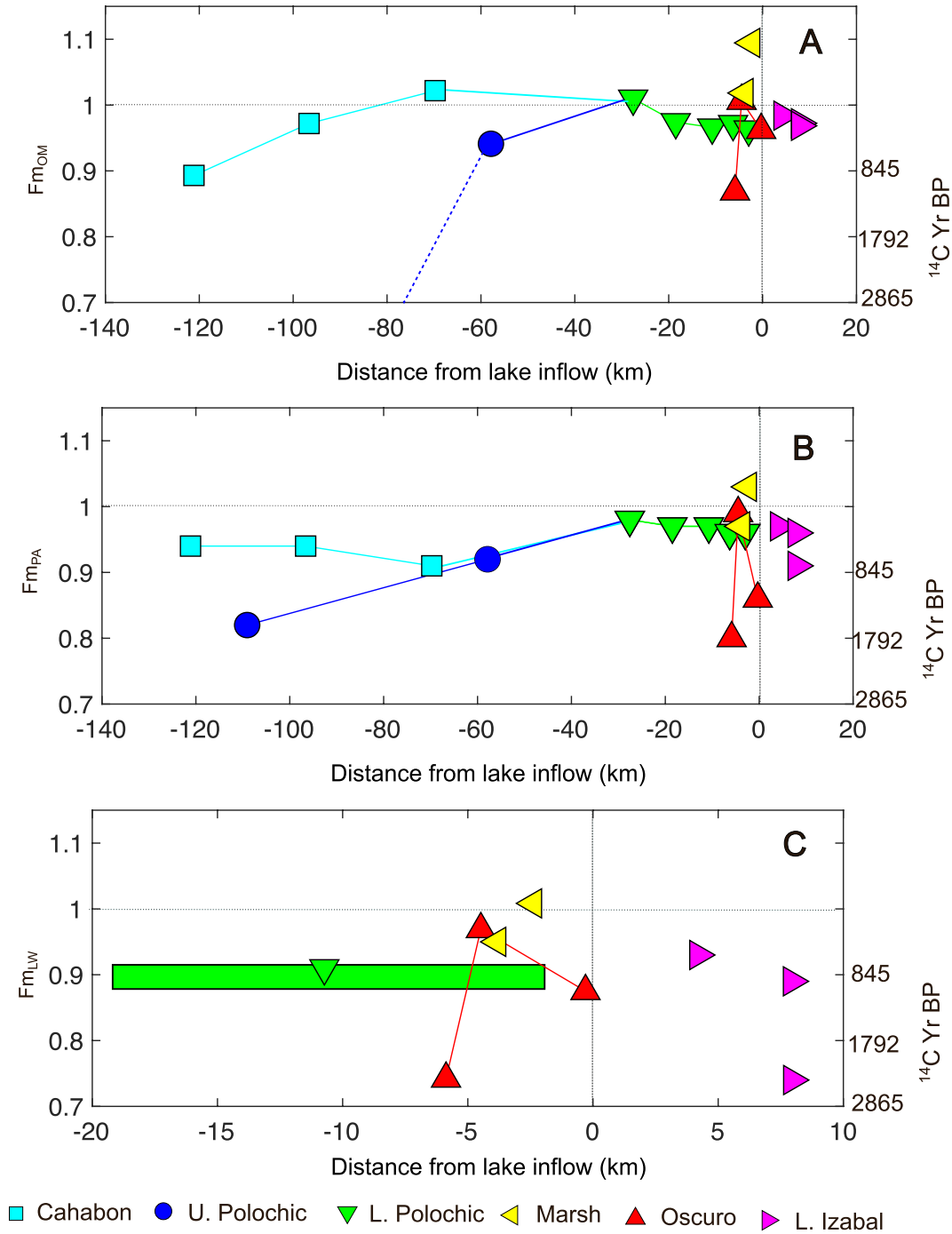

Figure 3. Fm_{OM} (a), Fm_{PA} (b), and Fm_{LW} as a function of distance from the river mouths entering Lake Izabal. Negative distances are upstream of the lake mouth, and positive distances are offshore of the lake. Dotted blue line in (a) indicates the trend toward anomalous sample LIM-41. The *x*-axis dimensions are different in (c) because there were insufficient leaf waxes in the Upper Polochic and Cahabón sediments. Samples in the lower Polochic that were combined for a leaf-wax ^{14}C measurement are shown as a rectangle spanning the location of the samples. The analytical uncertainty is smaller than the symbol size for all data.

($n = 4$) −26.4 ± 1.2‰; DPW ($n = 5$) −27.4 ± 1.1‰; PM ($n = 2$) −30.25 ± 0.35‰; OW ($n = 3$) −29.6 ± 0.23‰; and LI ($n = 3$) −30.9 ± 0.46‰ (Figure 2b).

For palmitic acid, $\delta^{13}C$ values ($\delta^{13}C_{PA}$) ranged widely from −37.1‰ to −30.5‰, with a catchment-wide average of −34.1 ± 2‰ (Table 1). The mean $\delta^{13}C_{PA}$ values for each subregion are: UPW ($n = 1$) −33.2‰; DPW ($n = 3$)

−31.7 ± 1‰; PM (n = 1) −35.4‰; OW (n = 3) −34.8 ± 0.3‰; LI (n = 3) −36.2 ± 0.8‰ (Figure 2c). We focus on weighted average $\delta^{13}C$ values for the long-chain n-alkanoic acids ($\delta^{13}C_{LW}$) (Table 1). $\delta^{13}C_{LW}$ values span a smaller range from −34.8 to −32.5‰, with a catchment wide average of −33.7 ± 0.72‰. The mean $\delta^{13}C_{LW}$ values for each subregion are: Upriver PW (n = 1) −33.8; Downriver PW (n = 3) −33.1 ± 0.5‰; PM (n = 1) −33.7‰ (n = 1); OW (n = 3) −33.2 ± 0.3‰; LI (n = 3) −34.6 ± 0.2‰ (Figure 2d).

5. Discussion

5.1. Comparison of Fatty Acid and Bulk Organic Matter Radiocarbon Measurements

Overall, palmitic acid, leaf wax, and bulk OM Fm values are significantly correlated, indicating consistent spatial variability in mean age between these three fractions of OM (Figure 4). With a few exceptions, the pattern of relative ages is that bulk OM contains the youngest C, palmitic acid is intermediate in C age, and leaf waxes contain the oldest C. The mean ^{14}C age difference between bulk OM and palmitic acid is 224 ± 328 years, the mean ^{14}C age difference between bulk OM and leaf waxes is 721 ± 616 years, and the mean ^{14}C age difference between palmitic acid and leaf waxes is 439 ± 501 years. The pattern of leaf waxes being older than palmitic acid is consistent with leaf waxes being relatively recalcitrant molecules that are stored in soils for longer periods of time, whereas palmitic acid is a more labile molecule that is more likely to be sourced from modern carbon, including through aquatic primary productivity. This relative age difference between leaf waxes and palmitic acid has been observed previously in soils, lake sediments, and deltaic sediments (French et al., 2018; Grant et al., 2022; Yamamoto et al., 2020), although the opposite pattern has been observed in a lake with a ^{14}C depleted dissolved inorganic carbon reservoir (Makou et al., 2018). Differences between leaf waxes and bulk OM in the literature are more variable, and depend in large part on the relative abundance of highly recalcitrant or petrogenic OC in different sedimentary basins, which can contribute to old bulk OM (French et al., 2018; Galy & Eglinton, 2011; Kusch et al., 2010; Yamamoto et al., 2020). Our data suggest that these fossil or old carbon reservoirs are not a major component of sedimentary OM in the Izabal Basin, despite the presence of mountain belts containing sedimentary rocks surrounding the basin, with the possible exception of the anomalous sample LIM-41.

It is unexpected that palmitic acid is almost always older than bulk OM in our samples, as it is a relatively labile molecule produced by a wide range of organisms, including plants, soil and aquatic heterotrophic microbes, and aquatic primary producers. It is possible that the relatively old ^{14}C ages for palmitic acid reflect incorporation of ^{14}C depleted DIC by aquatic photosynthetic organisms. However, this is unlikely for two reasons: (a) The upper PW and OW ecosystems, where Fm_{PA} is lowest, are characterized by dark and turbid waters that would act to limit aquatic primary productivity (Figure S1 in Supporting Information S1); and (b) we do not observe a negative relationship between Fm and $\delta^{13}C$ for any carbon fraction, which would be expected if photosynthetic organisms were incorporating dissolved carbonate that is enriched in ^{13}C and depleted in ^{14}C (Figure S6 in Supporting Information S1). However, more data on the ^{14}C of DIC and biomarkers specific to aquatic organisms would be needed to fully rule out this possibility.

Instead, we argue that the most likely explanation for the consistently aged ^{14}C signature of palmitic acid is that a significant amount of this molecule is derived from soil carbon reservoirs, most likely from soil microbial biomass. We observe a significant positive correlation between Fm_{PA} and bulk sediment OC:N ratios in the Polochic-Cahabón system specifically (i.e., subregions UPW and DPW; Figure 5a). While low sediment OC:N values are often interpreted to be an indicator of algal biomass, soil microbial biomass also contains very low OC:N ratios in the range of 6–12, and soil OM generally has low OC:N ratios similar to that observed in algae (Kirkby et al., 2011; Tipping et al., 2016). We infer that the observed correlation represents a mixing relationship between sediments that are rich in aged soil microbial biomass with low OC:N ratios in the upstream parts of the Polochic and Cahabón rivers, and sediments that are rich in contemporary algal and plant biomass in the downstream Polochic river. A study of Hawaiian subsoils from a similarly wet tropical environment found ^{14}C ages of palmitic acid that were younger than bulk soil OM, but consistently premodern (Fm_{PA} from 0.8 to 0.97) (Grant et al., 2022), implying that erosion of subsoils could contribute old palmitic acid to fluvial sediments.

The positive correlation between Fm_{OM} and both Fm_{PA} and Fm_{LW} (Figure 4) suggests that the inputs of aged OM, most likely dominantly from soils, are influencing bulk OM in the Polochic-Cahabón river sediments. This is not surprising given that aged OM is widely observed in river systems, including in the tropics (Galy & Eglinton, 2011;

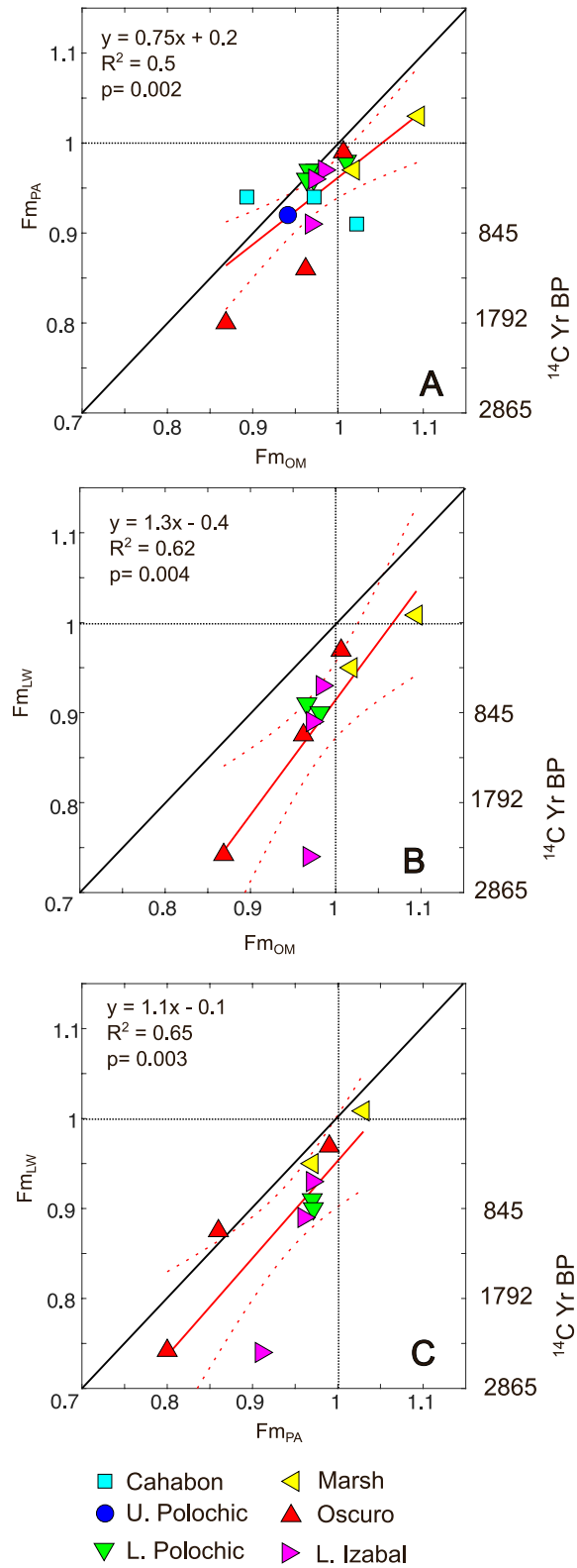

Figure 4. Scatter plots comparing (a) Fm_{OM} versus Fm_{PA}; (b) Fm_{OM} versus. Fm_{LW}; and (c) Fm_{PA} versus. Fm_{LW}. Solid black line indicates a 1:1 relationship. Red solid lines indicate linear regression relationships and dotted red lines indicate confidence intervals. Dashed line separates modern from pre-modern Fm values. The analytical uncertainty is smaller than the symbol size for all data.

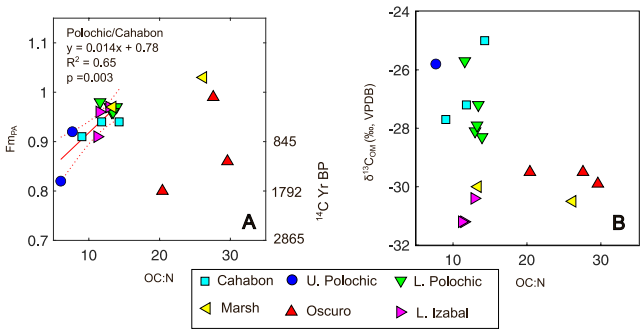

Figure 5. (a) Scatter plot comparing sediment OC:N ratios and Fm_{PA} values. Red solid and dotted lines indicate linear regression relationship and confidence intervals for samples from the Polochic-Cahabón river system only. (b) Scatter plot comparing sediment OC:N ratios and $\delta^{13}C_{OM}$. The analytical uncertainty is smaller than the symbol size for all data.

Schefuß et al., 2016; Wei et al., 2021). The generally younger ^{14}C age of OM relative to palmitic acid suggests that there is also a significant component of labile and rapidly cycling OM contained in bulk sediment OM that is not reflected by palmitic acid, possibly including non-lipid molecules with shorter soil residence times, such as cellulose or lignin (Feng et al., 2013; Jia et al., 2019). It is noteworthy that this relationship is not observed in the UPW sediments, where Fm_{OM} and Fm_{PA} appear to be negatively correlated (Figure 4a). We suggest this might be caused by varying inputs of petrogenic carbon. Variable inputs of eroded sedimentary rock could lead to low Fm_{OM} but would not be expected to influence Fm_{PA} since palmitic acid would not be preserved in million-year old sedimentary rocks (Galy & Eglinton, 2011).

5.2. Soil Erosion-Controlled Export of Aged Organic Matter in the Polochic-Cahabón River System

In the Polochic-Cahabón river network, we observe a clear spatial pattern in the age of OM in sediments, specifically for Fm_{OM} and Fm_{PA}, wherein sediments in the UPW contain older C than sediments in the downstream lowland river (LPW) (Figures 3a and 3b). This difference is especially pronounced for Fm_{PA}, where the lower Polochic samples are consistently younger than the upstream samples. For Fm_{OM} the difference is less clear, with the youngest OM near the confluence of the Cahabón and Polochic, and somewhat older OM downstream of the confluence. Based on our interpretations of the origin of pre-modern palmitic acid, we infer that the old OM found in upstream sediments is derived from eroded soil OM, as well as a potential contribution of petrogenic carbon from eroding sedimentary rocks for bulk OM. We also observe possible differences between the Polochic and Cahabón rivers, although given the small sample sizes these differences are only suggestive. In general, we would expect a greater contribution of eroded soil and petrogenic carbon in the Polochic given its steeper relief, and this is consistent with the overall older ages of OM and palmitic acid in this river, including the anomalously old bulk OM age from LIM-41.

In the lowland DPW, the generally higher values for Fm_{PA} and Fm_{OM} likely indicate inputs of local modern plant and algal biomass that dilute the old carbon exported from eroding highland soils. It is also possible that fresh plant litter from highland ecosystems is flushed into the lowland river but is not retained in upstream sediments. However, almost all samples in DPW sediments have Fm values below 1, indicating that a substantial component of aged OM transported from highland soils remains present in the lowland river. This is in contrast to samples from marsh sediments outside of the main river network, for which Fm values of all carbon fractions are higher (Figures 3 and 4), indicating that local primary production in the absence of the influence of exported upstream sediments leads to a predominance of modern C. Based on the simple mixing model described in Section 3.6, we estimate that approximately 39% of bulk OM and palmitic acid and 61% of leaf waxes at the mouth of the Polochic River are derived from aged soil OM. For bulk OM, our model does not account for the possible contribution of petrogenic carbon, and therefore is likely an overestimate of pre-aged biogenic soil OM inputs. For palmitic acid and leaf waxes, the applied Fm endmember for eroded soil may be too high, since eroded soil OM likely contains a continuum of different ages and we do not have a direct measurement of this value. Therefore, for these fractions the estimated contribution from eroded soil may also be an overestimate. Despite this uncertainty, we infer that a significant proportion of sedimentary OM transported by this river is derived from aged soil OM.

Our results indicate that the youngest bulk OM ages occur near the confluence of the rivers, and that Fm_{OM} decreases further downstream. We suggest this may reflect deposition of particulate plant biomass in this region where the elevation gradient rapidly decreases, leading to a decrease in stream power and deposition of larger particles in fluvial sediments. This is consistent with other studies indicating that fresh plant material is flushed from high-energy upstream environments and deposited in low-energy streambeds or lake sediments (Dalzell et al., 2007; Douglas et al., 2022; Smith et al., 2013). The sample closest to the confluence contains a significantly higher bulk $\delta^{13}C$ value than other LPW sediments (Figure 2b), consistent with an accumulation of biomass from upstream ecosystems with higher $\delta^{13}C$ values, including possible input from maize agricultural fields and other C_4 plants that are common in the upstream regions of both the Polochic and Cahabón rivers (Figure S2 in Supporting Information S1).

5.3. Export of Old Plant Carbon Preserved in Wetlands in the Rio Oscuro Catchment

In samples from the OW we observe a markedly different pattern of aged carbon export, with two samples (LIM-15 and LIM-17) expressing notably low values for Fm_{PA}, Fm_{LW}, and Fm_{OM} (Figure 3) despite much higher OC:N values than observed in the UPW and LPW sediments (Figure 2a), suggesting a predominance of plant biomass. While the data set for the OW is small, there is clearly substantial heterogeneity in the age of OM in this river, with sample LIM-16 containing much younger carbon across all three fractions. LIM-16 was collected at the confluence of two tributaries, and we infer that different tributaries of the OW are likely contributing OM of different ages. Sample LIM-17, collected near the mouth of the river, reflects an integrated sampling of the catchment, and is intermediate in terms of Fm values between the two upstream samples.

Overall, the data from the OW suggest a different mechanism for the export of aged OM from that observed in the Polochic-Cahabón catchment. The OW retains a higher amount of forest cover relative to the Polochic-Cahabón catchment and contains extensive wetlands, including forested swamps. This relatively undisturbed forest-swamp landscape likely preserves significant amounts of relatively undecomposed plant OM, especially in anoxic swamp sediments. We infer that this aged plant matter is gradually released into the river system, and exported downstream as sediments, where it mixes in varying degrees with more recent biomass.

Overall, based on comparison of river mouth sediments, this mechanism of old carbon release leads to the export of bulk OM that is similar in age to the larger Polochic-Cahabón river, but is older in terms of palmitic acid and leaf waxes. Based on our simple mixing model, we estimate that 29% of bulk OM, 61% of palmitic acid, and 56% of leaf waxes in sediments at the mouth of the Rio Oscuro are derived from aged soil carbon. The caveats to the mixing model discussed in Section 4.2 also apply here, although petrogenic OM is less likely to be an important contribution. One intriguing aspect of the OW data is that the river mouth sample (LIM-17) is the only sample in the data set for which Fm_{PA} is lower than Fm_{LW} (Figure 4c). One possible explanation for this result is that old plant biomass exported from swamps is being consumed by heterotrophic microbes within the fluvial network, leading to low ^{14}C in microbial biomass and palmitic acid at the river mouth. Based on measurements of fluvial discharge and OM concentrations (Brinson, 1976), the OM flux from the OW is about half that of the PW. Therefore, the contribution of pre-aged carbon from the OW to the overall lake basin could be significant. However, as discussed below, the lake sediment geochemical characteristics are overall more similar to the PW sediments.

5.4. Lake Izabal Sediment Organic Matter Contains Substantial Pre-Aged Carbon

All three lake sediment samples contain pre-modern Fm values for the three carbon fractions, indicating that a significant amount of aged carbon is buried within lake sediments. Fm_{OM} values for the three samples span a relatively small range (0.97–0.98), and are close to but slightly younger than sediments from the river mouths (both 0.96). This implies that bulk OM input to lake sediments is consistent with a predominantly fluvial source but is likely diluted with a component of autochthonous biomass containing younger carbon. For two samples (LIM-7 and LIM-11) Fm_{PA} and Fm_{LW} are also similar to values from the river mouths, but a third sample (LIM-9) contains much older carbon in these two fractions (Figure 3). This sample is especially anomalous in terms of the very low Fm_{LW} value (0.74), which is an outlier in regression plots of Fm_{LW} versus Fm_{PA} and Fm_{OM} (Figures 4b and 4c). This implies a mechanism for deposition of aged leaf waxes in lake sediments that is distinct from processes occurring in fluvial sediments. One possibility is that this sample reflects hydrodynamic processes that concentrate aged leaf waxes in offshore sediments, for example, greater ballasting of old leaf wax molecules associated with soil minerals or aggregates, which is consistent with other findings from fluvial and deltaic systems (Vonk et al., 2010b). We infer that the low Fm_{LW} in this sample is not the result of resuspension and within-basin transport of lake sediment OM, since we expect that process to affect all fractions of OM similarly. Overall, the variability in ^{14}C between these samples points to pronounced within-lake spatial variability in lake sediment OM age, and likely in OM source. Spatial heterogeneity in sediment OM isotopic composition has been observed in some other systems (Bovee & Pearson, 2014; Douglas et al., 2022; Murase & Sakamoto, 2000; Taylor et al., 2015), but is not typically incorporated in studies of inland water sediment C burial.

The lake sediment samples contain low OC:N ratios, similar to those found in the PW sediments, in contrast to the higher values observed in OW sediments (Figure 5). The combination of pre-modern carbon and low OC:N values in these samples suggests an important component of eroded soil OM, similar to the samples found in the DPW. However, the $\delta^{13}C$ values for the lake sediment samples are lower than any of the other samples we

analyzed, implying a distinctive source of OM to these samples (Figures 2 and 5b). One possibility is that this indicates input of phytoplankton or aquatic plant OM within the lake. For example, emergent aquatic plants in Guatemalan lakes tend to have very low leaf wax $\delta^{13}C$ values (Douglas et al., 2014). Our results suggest that autochthonous OM is mixing with allochthonous OM that is older than the mean age observed in these samples. Based on our simple mixing model, we calculate that across the three lake sediment samples approximately 30%–35% of bulk lake sediment OM, 35%–60% of lake sediment palmitic acid, and 52%–100% of leaf waxes are derived from eroded pre-aged soil carbon. The same uncertainties and caveats discussed in Section 4.2 apply to these estimates. The high contribution of pre-aged leaf waxes estimated here is consistent with previous estimates based on in-depth studies of coastal and lacustrine sediment cores (Douglas et al., 2014; French et al., 2018; Vonk et al., 2019).

Overall, our surface sediment data suggest mean transit times of hundreds to thousands of years for OM deposited in Lake Izabal. This is important both for understanding the source of OM buried in the lake, and for interpreting OM and biomarker-based paleoclimate proxy records in lake sediment cores. Our data are consistent with similar studies showing soil carbon-derived leaf waxes with centennial to millennial transit times being buried in lake sediments (Aichner et al., 2021; Douglas et al., 2014; Freimuth et al., 2021; Gierga et al., 2016; Kruger et al., 2022). Our data from Lake Izabal provide evidence that pre-aged leaf waxes can be an important input to non-karst tropical lake basins. There is one other study of leaf wax ^{14}C ages from a tropical tectonic lake basin, Lake Malawi, which focused on *n*-alcohols (Kruger et al., 2022). The *n*-alkanoic acids in Lake Izabal sediments are consistently older than the *n*-alcohols measured in Lake Malawi sediments (Fm between 0.95 and 1.1). This difference may either be because of the less recalcitrant nature of *n*-alcohols (Kusch et al., 2021), or smaller inputs of aged soil carbon in the Lake Malawi catchment. Since we saponified the sample extracts, the ^{14}C data represents both free and bound fatty acids, which is typical in compound specific radiocarbon studies. Analyses of free fatty acids alone could potentially produce different results, and this would be an interesting avenue for future research, especially in regard to interpreting leaf wax paleoenvironmental proxies.

The relatively wide range of leaf wax ages in the fluvial and lacustrine sediments suggests that the observed lake sediment leaf wax ^{14}C ages reflect a mixture of leaf waxes from carbon reservoirs with widely differing residence times. In theory, this should lead to mixing of stable isotope values from different sources, and most likely strong attenuation of stable isotope records in sediment cores (Douglas et al., 2014; French et al., 2018). This prediction is complicated, however, by the observation of depleted $\delta^{13}C$ values in the lake sediment leaf waxes relative to other samples, indicating that there is a source of leaf waxes that is not represented by the fluvial sediment samples. Given the clear indication of aged plant waxes in this tropical lake, and in others (Douglas et al., 2014; Kruger et al., 2022), gaining a better understanding of how the input of this aged material affects leaf wax isotopic paleoclimate proxy data is important for this field of study (Inglis et al., 2022).

5.5. Implications for Catchment-Scale Organic Matter Export and Burial

The LIB is in a high-precipitation, high-temperature tropical environment where soil residence times would be expected to be relatively low on a global scale. Empirical models based on global data compilations predict catchment scale ^{14}C ages of leaf waxes of about 1,000 years in this type of climate (Eglinton et al., 2021), which is consistent with the mean age of our leaf wax data (975 $\pm$ 829 ^{14}C years, 1σ standard deviation). However, interpretation of this mean residence time is complicated by the high degree of variability in ^{14}C content we observe across the sampled fluvial networks. We found evidence for two distinct modes of aged soil C export to the lake basin. The first is old soil C associated with low %TOC and low OC:N ratios in the PW, which we infer is comprised of mineral-associated OM released via soil erosion from largely deforested upland areas. The second is old soil C associated with high %TOC and high OC:N ratios in the smaller OW that drains largely intact forests and swamps, which we infer is comprised of plant biomass that is gradually exported from waterlogged and anaerobic peat soils with limited biodegradation. Our lake sediment data suggest that carbon buried in lake sediments is dominantly influenced by mineral-associated OM exported by the first mechanism, although the provenance of OM in lake sediments is not fully represented by input from either the PW or OW fluvial sediments.

The consistently pre-modern Fm_{PA} values in the catchment sediments imply that there is a substantial export of pre-aged short-chain fatty acids from catchment soils, in addition to more recalcitrant molecules like leaf waxes. We infer that pre-aged palmitic acid is primarily derived from soil microbes, but additional possible sources include plant biomass from soils and aquatic heterotrophic microbes that consume aged carbon within the fluvial

network. Regardless of the source of palmitic acid, the relatively low Fm_{PA} values observed in this system imply an important role for physical protection of soil OM, including relatively labile fatty acids, in the export of aged carbon in fluvial systems (Marín-Spiotta et al., 2014). We argue that additional CSRA studies of palmitic acid and other short-chain fatty acids would be valuable to better understand aged labile C export in river systems.

Our results point to the key role of wetlands in the Lake Izabal catchment in controlling and modulating the export of aged carbon to lake sediments, similar to inferences for other tropical river basins (Moore et al., 2013; Schefuß et al., 2016). However, the effect of wetlands in the Izabal catchment in controlling aged carbon export differs between the Polochic and Oscuro river catchments. The productive wetlands of the Lower Polochic appear to primarily influence carbon exports by adding modern carbon from wetland plants and planktonic communities that dilute the aged soil carbon being supplied from eroding highland soils (Figure 3). In contrast, the forests and swamps of the OW appear to build up substantial reservoirs of aged soil OM in the form of undecomposed plant biomass, which is then gradually exported by the Rio Oscuro. The causes of this difference are not clear from our analysis. However, we suggest that the greater annual discharge of the PW, which is about an order of magnitude larger than the Rio Oscuro (Brinson, 1976), may play an important role. The relatively lower discharge of the Rio Oscuro may reduce flushing of OM in wetlands and allow for the buildup of OM with longer residence times.

Overall, our data imply that there is substantial export of aged soil carbon within the LIB, leading to a pre-modern bulk OM signal in most sediment samples despite the warm, wet, and productive environment. This is consistent with other studies in tropical river systems that find evidence for an important pre-modern component of fluvial sediment or particulate OM (Lin et al., 2021; Mayorga et al., 2005; Schefuß et al., 2016; Wei et al., 2021). Given the similar distribution of OM ages in fluvial and lake sediments, we suggest that this pre-aged OM derived from soils is largely being buried in sediments and is not being widely mineralized during fluvial transport. This transport of aged OM represents a transfer of millennial-aged carbon from one stable reservoir in soils to another stable reservoir in lake sediments. Better understanding of this transfer is critical for quantifying freshwater sediment carbon burial, and the extent to which it is independent of, or an extension of soil carbon storage (Berhe et al., 2007; Tan et al., 2020). In addition, stratigraphic data from lake sediment cores comparing the ^{14}C ages of FAMEs, bulk OM, and/or plant macrofossils can be informative in understanding how aged soil carbon burial in lake sediments varies in response to climatic and anthropogenic environmental change (Douglas et al., 2018; Gierga et al., 2016; Nakamura et al., 2016; Obrochta et al., 2018). The tropics are an important focus for this research since the fate of large carbon reservoirs in tropical biomass and soils is critical for understanding long-term carbon-cycling, the carbon-cycle impacts of deforestation and soil erosion, and the efficacy of biospheric carbon sequestration strategies (Albrecht & Kandji, 2003; Campo & Merino, 2016; Dialynas et al., 2016). Our study did not explicitly control for land use, but we observe roughly similar export of old carbon from the largely deforested Polochic catchment and the relatively undisturbed Oscuro catchment, albeit with different modes of old carbon export. This highlights that both disturbed and undisturbed tropical landscapes have the potential to release aged carbon. More focused research is needed to investigate the effects of land use change on this process.

6. Conclusions

We find that three carbon fractions, bulk sediment OM, palmitic acid, and long-chain *n*-alkanoic acids or leaf waxes, are dominantly pre-modern in fluvial and lake sediments of the Lake Izabal catchment, with ^{14}C ages ranging from 130 to 2,500 years, indicating an important input of aged OM into the sedimentary carbon reservoir in this tropical lake basin. Our results point to two distinct mechanisms for the release of aged carbon from catchment soils. First, the export of old soil C through erosion from deforested upland regions with steep relief, associated with low %TOC and low OC:N ratios in sediments; and second, the release of undegraded aged plant biomass C from swamps and other C-rich soils in undisturbed forests, associated with high %TOC and high OC:N ratios in sediments. We infer that the first mechanism provides most aged OM to lake sediments, although the provenance of lake sediment OM is complicated by depleted $\delta^{13}C$ values that are outside the range of values observed in fluvial sediments. The presence of pre-modern palmitic acid in almost all sediment samples points to an important contribution of millennial cycling C reservoirs, most likely in soils, to labile short-chain fatty acids in sediments. We infer that preservation of aged palmitic acid is probably facilitated in large part by mineral protection of soil OM, including microbial biomass, as supported by a positive correlation between sediment OC:N ratios and Fm_{PA} in the Polochic-Cahabón watershed. Leaf wax ages in lake sediments are highly variable and are either similar to or older than ages observed in fluvial sediments. This implies that aged leaf waxes

transported by rivers contribute to leaf waxes preserved in lake sediment records, and that this input of aged leaf waxes will influence paleoclimate records based on leaf wax isotopic data. Overall, our results point to a significant input of aged soil carbon into the sediments of a large tropical lake, implying an important transfer from one long-term carbon reservoir to another.

Global Research Collaboration Statement

Field sampling for this project was carried out within the scope of a long-term research program in the Lake Izabal basin (LIB) led by co-author Jonathan Obrist-Farner, who is a Guatemalan citizen based in the USA. This research program involves intensive collaborations with local scientists and environmental NGOs and governmental agencies to better understand the environment, past climate change, and natural hazards in the LIB. The local partners involved in this work are the Defensores de la Naturaleza, an NGO seeking to protect the natural environment of the LIB and the biodiverse Polochic wetlands, and the Autoridad Para el Manejo Sustentable de la Cuenca del Lago de Izabal y Rio Dulce (AMASURLI), a regional environmental authority under the direction of the Ministerio de Ambiente y Recursos Naturales. Members of Defensores de la Naturaleza were instrumental in collecting the samples for this project in 2017. Two of the co-authors (JOF, PMJD) are part of the leadership of the Lake Izabal Basin Research Endeavor (LIBRE), an international continental scientific drilling project that will provide major investment in infrastructure, scientific training, employment, and education in the communities surrounding Lake Izabal. This article forms part of the preliminary research that will support the LIBRE project.

Data Availability Statement

All of the data analyzed in this study are available as Tables S1–S3 in Supporting Information S2 in the open access data repository Figshare (https://doi.org/10.6084/m9.figshare.22557379) (Parker et al., 2023).

Acknowledgments
This research was funded by NSF Postdoctoral Research Fellowship 1952645 to WGP, by National Science Foundation Grant EAR-2029102 to JOF, and by NSERC Discovery Grant 2017-03902 and McGill Start-Up Funds to PMJD. Support was also provided by Natural Resources Canada's (NRCan's) Environmental Geoscience Program. The authors thank Oscar Nuñez, Heidy Garcia, Elmer Tun Pana, Noe Hernandez, and Defensores de la Naturaleza who provided lake access and assistance with sediment sampling. We also thank Thi Hao Bui for assistance with sample preparation and analysis at McGill University.

References

Ahad, J. M., & Pakdel, H. (2013). Direct evaluation of in situ biodegradation in Athabasca oil sands tailings ponds using natural abundance radiocarbon. *Environmental Science & Technology*, *47*(18), 10214–10222. https://doi.org/10.1021/es402302z

Ahad, J. M., Pakdel, H., Savard, M. M., Simard, M.-C., & Smirnoff, A. (2012). Extraction, separation, and intramolecular carbon isotope characterization of Athabasca oil sands acids in environmental samples. *Analytical Chemistry*, *84*(23), 10419–10425. https://doi.org/10.1021/ac302680y

Aichner, B., Gierga, M., Stolz, A., Mętrak, M., Wilk, M., Suska-Malawska, M., et al. (2021). Do radiocarbon ages of plant wax biomarkers agree with 14CTOC/OSL-based age models in an arid high-altitude lake system? *Radiocarbon*, *63*(6), 1575–1590. https://doi.org/10.1017/rdc.2021.78

Albrecht, A., & Kandji, S. T. (2003). Carbon sequestration in tropical agroforestry systems. *Agriculture, Ecosystems & Environment*, *99*(1–3), 15–27. https://doi.org/10.1016/s0167-8809(03)00138-5

Anderson, N. J., Heathcote, A., & Engstrom, D. (2020). Anthropogenic alteration of nutrient supply increases the global freshwater carbon sink. *Science Advances*, *6*(16), eaaw2145. https://doi.org/10.1126/sciadv.aaw2145

Bartole, R., Lodolo, E., Obrist-Farner, J., & Morelli, D. (2019). Sedimentary architecture, structural setting, and Late Cenozoic depocentre migration of an asymmetric transtensional basin: Lake Izabal, eastern Guatemala. *Tectonophysics*, *750*, 419–433. https://doi.org/10.1016/j.tecto.2018.12.004

Berhe, A. A., Harte, J., Harden, J. W., & Torn, M. S. (2007). The significance of the erosion-induced terrestrial carbon sink. *BioScience*, *57*(4), 337–346. https://doi.org/10.1641/b570408

Bonis, S., Bohnenberger, O., & Dengo, G. (1970). *Geologic map of Guatemala, 1: 50,000*. Instituto Geográfico Nacional.

Bourque, R. D., Douglas, P. M., & Larsson, H. C. (2021). Changes in terrestrial ecosystems across the Cretaceous-Paleogene boundary in western Canada inferred from plant wax lipid distributions and isotopic measurements. *Palaeogeography, Palaeoclimatology, Palaeoecology*, *562*, 110081. https://doi.org/10.1016/j.palaeo.2020.110081

Bovee, R., & Pearson, A. (2014). Strong influence of the littoral zone on sedimentary lipid biomarkers in a meromictic lake. *Geobiology*, *12*(6), 529–541. https://doi.org/10.1111/gbi.12099

Brinson, M. M. (1976). Organic matter losses from four watersheds in the humid tropics 1. *Limnology and Oceanography*, *21*(4), 572–582. https://doi.org/10.4319/lo.1976.21.4.0572

Brinson, M. M., Brinson, L. G., & Lugo, A. E. (1974). The gradient of salinity, its seasonal movement, and ecological implications for the Lake Izabal—Rio Dulce ecosystem, Guatemala. *Bulletin of Marine Science*, *24*(3), 533–544.

Campo, J., & Merino, A. (2016). Variations in soil carbon sequestration and their determinants along a precipitation gradient in seasonally dry tropical forest ecosystems. *Global Change Biology*, *22*(5), 1942–1956. https://doi.org/10.1111/gcb.13244

Copard, Y., Eyrolle, F., Grosbois, C., Lepage, H., Ducros, L., Morereau, A., et al. (2022). The unravelling of radiocarbon composition of organic carbon in river sediments to document past anthropogenic impacts on river systems. *Science of the Total Environment*, *806*, 150890. https://doi.org/10.1016/j.scitotenv.2021.150890

Coplen, T. B. (2011). Guidelines and recommended terms for expression of stable-isotope-ratio and gas-ratio measurement results. *Rapid Communications in Mass Spectrometry*, *25*(17), 2538–2560. https://doi.org/10.1002/rcm.5129

Dalzell, B. J., Filley, T. R., & Harbor, J. M. (2007). The role of hydrology in annual organic carbon loads and terrestrial organic matter export from a midwestern agricultural watershed. *Geochimica et Cosmochimica Acta*, *71*(6), 1448–1462. https://doi.org/10.1016/j.gca.2006.12.009

Dean, W. E., & Gorham, E. (1998). Magnitude and significance of carbon burial in lakes, reservoirs, and peatlands. *Geology*, *26*(6), 535–538. https://doi.org/10.1130/0091-7613(1998)026<0535:masocb>2.3.co;2

Dialynas, Y. G., Bastola, S., Bras, R. L., Marin-Spiotta, E., Silver, W. L., Arnone, E., & Noto, L. V. (2016). Impact of hydrologically driven hillslope erosion and landslide occurrence on soil organic carbon dynamics in tropical watersheds. *Water Resources Research*, *52*(11), 8895–8919. https://doi.org/10.1002/2016wr018925

Diefendorf, A. F., & Freimuth, E. J. (2017). Extracting the most from terrestrial plant-derived n-alkyl lipids and their carbon isotopes from the sedimentary record: A review. *Organic Geochemistry*, *103*, 1–21. https://doi.org/10.1016/j.orggeochem.2016.10.016

Douglas, P. M., Pagani, M., Eglinton, T. I., Brenner, M., Curtis, J. H., Breckenridge, A., & Johnston, K. (2018). A long-term decrease in the persistence of soil carbon caused by ancient Maya land use. *Nature Geoscience*, *11*(9), 645–649. https://doi.org/10.1038/s41561-018-0192-7

Douglas, P. M., Pagani, M., Eglinton, T. I., Brenner, M., Hodell, D. A., Curtis, J. H., et al. (2014). Pre-aged plant waxes in tropical lake sediments and their influence on the chronology of molecular paleoclimate proxy records. *Geochimica et Cosmochimica Acta*, *141*, 346–364. https://doi.org/10.1016/j.gca.2014.06.030

Douglas, P. M., Stratigopoulos, E., Park, S., & Keenan, B. (2022). Spatial differentiation of sediment organic matter isotopic composition and inferred sources in a temperate forest lake catchment. *Chemical Geology*, *603*, 120887. https://doi.org/10.1016/j.chemgeo.2022.120887

Duarte, E., Obrist-Farner, J., Correa-Metrio, A., & Steinman, B. A. (2021). A progressively wetter early through middle Holocene climate in the eastern lowlands of Guatemala. *Earth and Planetary Science Letters*, *561*, 116807. https://doi.org/10.1016/j.epsl.2021.116807

Eglinton, T. I., Galy, V. V., Hemingway, J. D., Feng, X., Bao, H., Blattmann, T. M., et al. (2021). Climate control on terrestrial biospheric carbon turnover. *Proceedings of the National Academy of Sciences*, *118*(8), e2011585118. https://doi.org/10.1073/pnas.2011585118

Feng, X., Benitez-Nelson, B. C., Montluçon, D. B., Prahl, F. G., McNichol, A. P., Xu, L., et al. (2013). 14C and 13C characteristics of higher plant biomarkers in Washington margin surface sediments. *Geochimica et Cosmochimica Acta*, *105*, 14–30. https://doi.org/10.1016/j.gca.2012.11.034

Fisher, M. M., Brenner, M., & Reddy, K. (1992). A simple, inexpensive piston corer for collecting undisturbed sediment/water interface profiles. *Journal of Paleolimnology*, *7*(2), 157–161. https://doi.org/10.1007/bf00196870

Freimuth, E. J., Diefendorf, A. F., Lowell, T. V., Schartman, A. K., Landis, J. D., Stewart, A. K., & Bates, B. R. (2021). Centennial-scale age offsets of plant wax n-alkanes in Adirondack lake sediments. *Geochimica et Cosmochimica Acta*, *300*, 119–136. https://doi.org/10.1016/j.gca.2021.02.022

French, K. L., Hein, C. J., Haghipour, N., Wacker, L., Kudrass, H. R., Eglinton, T. I., & Galy, V. (2018). Millennial soil retention of terrestrial organic matter deposited in the Bengal Fan. *Scientific Reports*, *8*(1), 1–8. https://doi.org/10.1038/s41598-018-30091-8

Galy, V., & Eglinton, T. (2011). Protracted storage of biospheric carbon in the Ganges–Brahmaputra basin. *Nature Geoscience*, *4*(12), 843–847. https://doi.org/10.1038/ngeo1293

Gierga, M., Hajdas, I., van Raden, U. J., Gilli, A., Wacker, L., Sturm, M., et al. (2016). Long-stored soil carbon released by prehistoric land use: Evidence from compound-specific radiocarbon analysis on Soppensee lake sediments. *Quaternary Science Reviews*, *144*, 123–131. https://doi.org/10.1016/j.quascirev.2016.05.011

Grant, K. E., Galy, V. V., Haghipour, N., Eglinton, T. I., & Derry, L. A. (2022). Persistence of old soil carbon under changing climate: The role of mineral-organic matter interactions. *Chemical Geology*, *587*, 120629. https://doi.org/10.1016/j.chemgeo.2021.120629

Griffith, D. R., Martin, W. R., & Eglinton, T. I. (2010). The radiocarbon age of organic carbon in marine surface sediments. *Geochimica et Cosmochimica Acta*, *74*(23), 6788–6800. https://doi.org/10.1016/j.gca.2010.09.001

Hein, C. J., Usman, M., Eglinton, T. I., Haghipour, N., & Galy, V. V. (2020). Millennial-scale hydroclimate control of tropical soil carbon storage. *Nature*, *581*(7806), 63–66. https://doi.org/10.1038/s41586-020-2233-9

Hernández, E., Obrist-Farner, J., Brenner, M., Kenney, W. F., Curtis, J. H., & Duarte, E. (2020). Natural and anthropogenic sources of lead, zinc, and nickel in sediments of Lake Izabal, Guatemala. *Journal of Environmental Sciences*, *96*, 117–126. https://doi.org/10.1016/j.jes.2020.04.020

Inglis, G. N., Bhattacharya, T., Hemingway, J. D., Hollingsworth, E. H., Feakins, S. J., & Tierney, J. E. (2022). Biomarker approaches for reconstructing terrestrial environmental change. *Annual Review of Earth and Planetary Sciences*, *50*(1), 369–394. https://doi.org/10.1146/annurev-earth-032320-095943

INSIVUMEH. (2022). *Ríos de Guatemala* (Vol. 2022). Inst. Nac. Sismol. Vulcanol. Meteorol. e Hidrol.

Jia, J., Feng, X., Pannatier, E. G., Wacker, L., McIntyre, C., van der Voort, T., et al. (2019). 14C characteristics of dissolved lignin along a forest soil profile. *Soil Biology and Biochemistry*, *135*, 407–410. https://doi.org/10.1016/j.soilbio.2019.06.005

Kirkby, C., Kirkegaard, J., Richardson, A., Wade, L., Blanchard, C., & Batten, G. (2011). Stable soil organic matter: A comparison of C: N: P: S ratios in Australian and other world soils. *Geoderma*, *163*(3–4), 197–208. https://doi.org/10.1016/j.geoderma.2011.04.010

Kruger, B. R., Werne, J. P., & Minor, E. C. (2022). Sediment organic matter compositional changes in a tropical rift lake as a function of water depth and distance from shore. *Organic Geochemistry*, *175*, 104527. https://doi.org/10.1016/j.orggeochem.2022.104527

Kusch, S., Mollenhauer, G., Willmes, C., Hefter, J., Eglinton, T. I., & Galy, V. (2021). Controls on the age of plant waxes in marine sediments–a global synthesis. *Organic Geochemistry*, *157*, 104259. https://doi.org/10.1016/j.orggeochem.2021.104259

Kusch, S., Rethemeyer, J., Schefuß, E., & Mollenhauer, G. (2010). Controls on the age of vascular plant biomarkers in Black Sea sediments. *Geochimica et Cosmochimica Acta*, *74*(24), 7031–7047. https://doi.org/10.1016/j.gca.2010.09.005

Lin, B., Liu, Z., Eglinton, T. I., Blattmann, T. M., Kandasamy, S., Haghipour, N., & Siringan, F. P. (2021). Organic matter compositions and loadings in river sediments from humid tropical volcanic Luzon Island of the Philippines. *Journal of Geophysical Research: Biogeosciences*, *126*(7), e2020JG006192. https://doi.org/10.1029/2020jg006192

Makou, M., Eglinton, T., McIntyre, C., Montluçon, D., Antheaume, I., & Grossi, V. (2018). Plant wax n-alkane and n-alkanoic acid signatures overprinted by microbial contributions and old carbon in meromictic lake sediments. *Geophysical Research Letters*, *45*(2), 1049–1057. https://doi.org/10.1002/2017gl076211

Marín-Spiotta, E., Gruley, K., Crawford, J., Atkinson, E., Miesel, J., Greene, S., et al. (2014). Paradigm shifts in soil organic matter research affect interpretations of aquatic carbon cycling: Transcending disciplinary and ecosystem boundaries. *Biogeochemistry*, *117*(2), 279–297. https://doi.org/10.1007/s10533-013-9949-7

Mayorga, E., Aufdenkampe, A. K., Masiello, C. A., Krusche, A. V., Hedges, J. I., Quay, P. D., et al. (2005). Young organic matter as a source of carbon dioxide outgassing from Amazonian rivers. *Nature*, *436*(7050), 538–541. https://doi.org/10.1038/nature03880

McCorkle, E. P., Berhe, A. A., Hunsaker, C. T., Johnson, D. W., McFarlane, K. J., Fogel, M. L., & Hart, S. C. (2016). Tracing the source of soil organic matter eroded from temperate forest catchments using carbon and nitrogen isotopes. *Chemical Geology*, *445*, 172–184. https://doi.org/10.1016/j.chemgeo.2016.04.025

Mendonça, R., Müller, R. A., Clow, D., Verpoorter, C., Raymond, P., Tranvik, L. J., & Sobek, S. (2017). Organic carbon burial in global lakes and reservoirs. *Nature Communications*, *8*(1), 1–7. https://doi.org/10.1038/s41467-017-01789-6

Moore, S., Evans, C. D., Page, S. E., Garnett, M. H., Jones, T. G., Freeman, C., et al. (2013). Deep instability of deforested tropical peatlands revealed by fluvial organic carbon fluxes. *Nature*, *493*(7434), 660–663. https://doi.org/10.1038/nature11818

Murase, J., & Sakamoto, M. (2000). Horizontal distribution of carbon and nitrogen and their isotopic compositions in the surface sediment of Lake. *Biwa: Limnology*, *1*(3), 177–184. https://doi.org/10.1007/s102010070004

Nakamura, A., Yokoyama, Y., Maemoku, H., Yagi, H., Okamura, M., Matsuoka, H., et al. (2016). Weak monsoon event at 4.2 ka recorded in sediment from Lake Rara, Himalayas. *Quaternary International*, *397*, 349–359. https://doi.org/10.1016/j.quaint.2015.05.053

Obrist-Farner, J., Brenner, M., Curtis, J. H., Kenney, W. F., & Salvinelli, C. (2019). Recent onset of eutrophication in Lake Izabal, the largest water body in Guatemala. *Journal of Paleolimnology*, *62*(4), 359–372. https://doi.org/10.1007/s10933-019-00091-3

Obrist-Farner, J., Brenner, M., Stone, J. R., Wojewódka-Przybył, M., Bauersachs, T., Eckert, A., et al. (2022). New estimates of the magnitude of the sea-level jump during the 8.2 ka event. *Geology*, *50*(1), 86–90. https://doi.org/10.1130/g49296.1

Obrist-Farner, J., Eckert, A., Locmelis, M., Crowley, J. L., Mota-Vidaure, B., Lodolo, E., et al. (2020). The role of the Polochic Fault as part of the North American and Caribbean Plate boundary: Insights from the infill of the Lake Izabal Basin. *Basin Research*, *32*(6), 1347–1364. https://doi.org/10.1111/bre.12431

Obrist-Farner, J., Steinman, B. A., Stansell, N. D., & Maurer, J. (2023). Incoherency in central american hydroclimate proxy records spanning the last millennium. *Paleoceanography and Paleoclimatology*, *38*(3). e2022PA004445. Portico. https://doi.org/10.1029/2022pa004445

Obrochta, S., Yokoyama, Y., Yoshimoto, M., Yamamoto, S., Miyairi, Y., Nagano, G., et al. (2018). Mt. Fuji Holocene eruption history reconstructed from proximal lake sediments and high-density radiocarbon dating. *Quaternary Science Reviews*, *200*, 395–405. https://doi.org/10.1016/j.quascirev.2018.09.001

Olson, D. M., Dinerstein, E., Wikramanayake, E. D., Burgess, N. D., Powell, G. V., Underwood, E. C., et al. (2001). Terrestrial ecoregions of the world: A new map of life on earth: A new global map of terrestrial ecoregions provides an innovative tool for conserving biodiversity. *BioScience*, *51*(11), 933–938. https://doi.org/10.1641/0006-3568(2001)051[0933:teotwa]2.0.co;2

Parker, W., Jason, M. E. A., Obrist-Farner, J., Keenan, B., & Douglas, P. M. J. (2023). Data for Distinct modes of aged soil carbon export in a large tropical lake basin identified using bulk and compound-specific radiocarbon analyses of fluvial and lacustrine sediment [Dataset]. Figshare. https://doi.org/10.6084/m9.figshare.22557379.v2

Regnier, P., Resplandy, L., Najjar, R. G., & Ciais, P. (2022). The land-to-ocean loops of the global carbon cycle. *Nature*, *603*(7901), 401–410. https://doi.org/10.1038/s41586-021-04339-9

Reimer, P. J. (2004). Intcal04: Terrestrial radiocarbon age calibration, 0-26 cal kyr BP. *Radiocarbon*, *46*(3), 1029–1058.

Sachse, D., Billault, I., Bowen, G. J., Chikaraishi, Y., Dawson, T. E., Feakins, S. J., et al. (2012). Molecular paleohydrology: Interpreting the hydrogen-isotopic composition of lipid biomarkers from photosynthesizing organisms. *Annual Review of Earth and Planetary Sciences*, *40*(1), 221–249. https://doi.org/10.1146/annurev-earth-042711-105535

Schefuß, E., Eglinton, T. I., Spencer-Jones, C. L., Rullkötter, J., Pol-Holz, D., Talbot, H. M., et al. (2016). Hydrologic control of carbon cycling and aged carbon discharge in the Congo River basin. *Nature Geoscience*, *9*(9), 687–690. https://doi.org/10.1038/ngeo2778

Schimmelmann, A., Qi, H., Coplen, T. B., Brand, W. A., Fong, J., Meier-Augenstein, W., et al. (2016). Organic reference materials for hydrogen, carbon, and nitrogen stable isotope-ratio measurements: Caffeines, n-alkanes, fatty acid methyl esters, glycines, L-valines, polyethylenes, and oils. *Analytical Chemistry*, *88*(8), 4294–4302. https://doi.org/10.1021/acs.analchem.5b04392

Smith, J. C., Galy, A., Hovius, N., Tye, A. M., Turowski, J. M., & Schleppi, P. (2013). Runoff-driven export of particulate organic carbon from soil in temperate forested uplands. *Earth and Planetary Science Letters*, *365*, 198–208. https://doi.org/10.1016/j.epsl.2013.01.027

Tan, Z., Leung, L. R., Li, H. Y., Tesfa, T., Zhu, Q., & Huang, M. (2020). A substantial role of soil erosion in the land carbon sink and its future changes. *Global Change Biology*, *26*(4), 2642–2655. https://doi.org/10.1111/gcb.14982

Taylor, Z. P., Horn, S. P., & Finkelstein, D. B. (2015). Assessing intra-basin spatial variability in geochemical and isotopic signatures in the sediments of a small neotropical lake. *Journal of Paleolimnology*, *54*(4), 395–411. https://doi.org/10.1007/s10933-015-9859-x

Tipping, E., Somerville, C. J., & Luster, J. (2016). The C: N: P: S stoichiometry of soil organic matter. *Biogeochemistry*, *130*(1), 117–131. https://doi.org/10.1007/s10533-016-0247-z

Turnbull, J. C., Mikaloff Fletcher, S. E., Brailsford, G. W., Moss, R. C., Norris, M. W., & Steinkamp, K. (2017). Sixty years of radiocarbon dioxide measurements at Wellington, New Zealand: 1954–2014. *Atmospheric Chemistry and Physics*, *17*(23), 14771–14784. https://doi.org/10.5194/acp-17-14771-2017

Uchikawa, J., Popp, B. N., Schoonmaker, J. E., & Xu, L. (2008). Direct application of compound-specific radiocarbon analysis of leaf waxes to establish lacustrine sediment chronology. *Journal of Paleolimnology*, *39*(1), 43–60. https://doi.org/10.1007/s10933-007-9094-1

Vonk, J. E., Drenzek, N. J., Hughen, K. A., Stanley, R. H., McIntyre, C., Montluçon, D. B., et al. (2019). Temporal deconvolution of vascular plant-derived fatty acids exported from terrestrial watersheds. *Geochimica et Cosmochimica Acta*, *244*, 502–521. https://doi.org/10.1016/j.gca.2018.09.034

Vonk, J. E., Sánchez-García, L., Semiletov, I., Dudarev, O., Eglinton, T., Andersson, A., & Gustafsson, Ö. (2010a). Molecular and radiocarbon constraints on sources and degradation of terrestrial organic carbon along the Kolyma paleoriver transect, East Siberian Sea. *Biogeosciences*, *7*(10), 3153–3166. https://doi.org/10.5194/bg-7-3153-2010

Vonk, J. E., Van Dongen, B. E., & Gustafsson, Ö. (2010b). Selective preservation of old organic carbon fluvially released from sub-Arctic soils. *Geophysical Research Letters*, *37*(11). https://doi.org/10.1029/2010gl042909

Wang, Z., Hoffmann, T., Six, J., Kaplan, J. O., Govers, G., Doetterl, S., & Van Oost, K. (2017). Human-induced erosion has offset one-third of carbon emissions from land cover change. *Nature Climate Change*, *7*(5), 345–349. https://doi.org/10.1038/nclimate3263

Wei, B., Mollenhauer, G., Hefter, J., Kusch, S., Grotheer, H., Schefuß, E., & Jia, G. (2021). The nature, timescale, and efficiency of riverine export of terrestrial organic carbon in the (sub) tropics: Insights at the molecular level from the Pearl River and adjacent coastal sea. *Earth and Planetary Science Letters*, *565*, 116934. https://doi.org/10.1016/j.epsl.2021.116934

Yamamoto, S., Miyairi, Y., Yokoyama, Y., Suga, H., Ogawa, N. O., & Ohkouchi, N. (2020). Compound-specific radiocarbon analysis of organic compounds from Mount Fuji proximal lake (Lake Kawaguchi) sediment, central Japan. *Radiocarbon*, *62*(2), 439–451. https://doi.org/10.1017/rdc.2019.158